PHYSICAL REVIEW B VOLUME 1, NUMBER 11 1 JUNE 1970

Electron-Magnon Interaction in Ferromagnetic Semiconductors*

Roy B. Woolsey† and Robert M. White

Department of Physics, Stanford University, Stanford, California 94305
(Received 30 January 1970)

The interaction between conduction electrons and localized moments in degenerate ferromagnetic semiconductors has been studied, assuming Bloch states for the conduction electrons and using the low-temperature spin-wave approximation. The finite-temperature Green's-function formalism has been used to obtain the real and imaginary parts of the electron and magnon self-energies, from which the electron and magnon energies, lifetimes, and specific heats have been calculated. It is found that the conduction-electron energy corrections as a function of electron wave vector behave quite differently for the two conduction-electron spin polarizations, and hence the effective masses and mobilities of up-moment conduction electrons are quite different from those of down-moment electrons. The electron lifetime associated with magnon scattering is short enough to make this a dominant contribution to the electron lifetime in magnetic semiconductors. The electronic specific heat in magnetic semiconductors is small owing to the small number of conduction electrons, and the correction to this specific heat arising from the electron-magnon interaction is also small. The magnon specific heat, on the other hand, is quite large in magnetic semiconductors at low temperatures, and as a result of the change in the magnon spectrum due to the electron-magnon interaction, there is a substantial correction to the magnon specific heat. All of these effects are quite strongly dependent on carrier concentration. Thus, by varying the doping it is possible to see dramatic changes in these effects.

I. INTRODUCTION

A great deal of effort is being made today to understand the physical properties of chalcogenide compounds involving transition-metal or rare-earth ions. Many of these compounds are magnetic, and an important problem is the relationship between their magnetic and electrical properties. One approach to this problem has been to study the optical properties of such materials in order to determine their band structure. Another approach has been to study the transport properties of doped samples. Such studies seem to indicate that magnetic polarons play an important role in the properties of these materials.

Much of the work on magnetic polarons in semiconductors has dealt with "small" polarons,[1] where one assumes *a priori* that the carriers are localized and interact only with those localized moments in their immediate vicinity. This paper, on the other hand, considers the properties of "large" polarons. We assume that the carriers may be described by Bloch waves that are much less affected by the impurity potentials than they are by their exchange interaction with the localized moments. The exchange interaction is taken to have the familiar *s-d* or *s-f* contact form. This model has recently been used to investigate the resistivity[2] and optical properties[3,4] of magnetic semiconductors. Also, we have previously investigated[5] the effect of this interaction on the effective mass of the carriers at zero temperature. This paper extends the previous work to finite temperatures, but temperatures still low enough to make a spin-wave description of magnetic fluctuations valid. We have also investigated the mobility due to magnon scattering. This complements the previous resistivity calculation[2] which, since it involves a quasistatic approximation, does not apply to low temperatures. We have also computed the correction to the specific heat arising from the electron-magnon interaction.

Similar studies have been made of the electron-magnon interaction in metals.[6,7] Ferromagnetic semiconductors, however, have the unique feature that below a certain carrier concentration – which depends upon the exchange splitting of the bands – all the carriers are completely spin polarized. The properties of these materials are strong functions of the carrier concentration, and we shall see this dramatically in the case of the electron effective mass, and electron and magnon lifetimes.

The calculations presented here have been carried out using a Green's-function formalism, which, for the most part, parallels that encountered in the electron-phonon problem.[8]

II. HAMILTONIAN

We consider a doped degenerate ferromagnetic semiconductor and first develop the Hamiltonian for the conduction-electron localized moment sys-

tem. We assume that the localized moments experience a ferromagnetic exchange interaction only with their Z nearest neighbors. The magnetic Hamiltonian is then

$$\mathcal{H}_{\text{mag}} = g\mu_B H \sum_{\vec{R}_i} S^z_{\vec{R}_i} - J \sum_{\vec{R}_i} \sum_{\vec{\delta}} \vec{S}_{\vec{R}_i} \cdot \vec{S}_{\vec{R}_i + \vec{\delta}} , \tag{1}$$

where g is the ionic g value, taken to be explicitly positive, μ_B is the Bohr magneton, H is the external magnetic field, assumed along the $+z$ direction, J is the exchange constant, and $\vec{\delta}$ is a vector to a nearest neighbor.

A parabolic energy band is assumed for the conduction electrons. The second-quantized electron Hamiltonian is

$$\mathcal{H}_{\text{elect}} = \sum_{\vec{k},\sigma} \epsilon_{\vec{k},\sigma} c^\dagger_{\vec{k},\sigma} c_{\vec{k},\sigma} , \tag{2}$$

where $$\epsilon_{\vec{k},\sigma} = (\hbar^2 k^2/2m) - \mu_B H\sigma . \tag{3}$$

Here $\sigma = +1$ for up conduction-electron moments and $\sigma = -1$ for down moments, and we have taken the g value of the conduction electrons to be 2.

The exchange part of the conduction-electron local moment interaction is represented by a spin-dependent contact potential.

$$\mathcal{H}_{\text{int}} = -I \sum_{\vec{R}_i} \sum_{\vec{r}_j} \vec{S}_{\vec{R}_i} \cdot \vec{s}_{\vec{r}_j} \Delta(\vec{R}_i - \vec{r}_j) , \tag{4}$$

where the sum over i refers to the local moments, and that over j to the conduction electrons. Second quantizing the electron part of this Hamiltonian gives

$$\mathcal{H}_{\text{int}} = -\frac{I}{2N} \sum_{\vec{k},\vec{k}',\vec{R}_i} e^{i(\vec{k}-\vec{k}')\cdot\vec{R}_i} (S^+_{\vec{R}_i} c^\dagger_{\vec{k}',+} c_{\vec{k},-} + S^-_{\vec{R}_i} c^\dagger_{\vec{k}',-} c_{\vec{k},+} + S^z_{\vec{R}_i} c^\dagger_{\vec{k}',-} c_{\vec{k},-} - S^z_{\vec{R}_i} c^\dagger_{\vec{k}',+} c_{\vec{k},+}) . \tag{5}$$

The S^z terms in $\mathcal{H}_{\text{int}}$ are treated in the random-phase approximation, and give rise to a splitting of the conduction band into up- and down-moment bands separated in energy by IS. The total Hamiltonian, Eqs. (1), (2), and (5), then becomes, up to a constant,

$$\mathcal{H} = \sum_{\vec{R}_i} \omega_0 S^z_{\vec{R}_i} + \sum_{\vec{k},\sigma} \tilde{\epsilon}_{\vec{k},\sigma} c^\dagger_{\vec{k},\sigma} c_{\vec{k},\sigma} - J \sum_{\vec{R}_i,\vec{\delta}} \vec{S}_{\vec{R}_i} \cdot \vec{S}_{\vec{R}_i + \vec{\delta}} - \frac{I}{2N} \sum_{\vec{k},\vec{k}',\vec{R}_i} e^{i(\vec{k}-\vec{k}')\cdot\vec{R}_i} (S^+_{\vec{R}_i} c^\dagger_{\vec{k}',+} c_{\vec{k},-} + S^-_{\vec{R}_i} c^\dagger_{\vec{k}',-} c_{\vec{k},+}) , \tag{6}$$

where $$\omega_0 = g\mu_B H + \frac{I}{2N} \sum_{\vec{k},\sigma} \langle n_{\vec{k},\sigma} \rangle \sigma \tag{7}$$

and $$\tilde{\epsilon}_{\vec{k},\sigma} = (\hbar^2 k^2/2m) - (\mu_B H + \tfrac{1}{2} IS)\sigma . \tag{8}$$

$\langle n_{\vec{k},\sigma} \rangle$ is the electron thermal occupation number. A term $(1/N)\sum_{\vec{q}} \langle n_{\vec{q}} \rangle$, where $\langle n_{\vec{q}} \rangle$ is the magnon thermal occupation number, has been neglected, as it is very small at low temperatures.

Before discussing the conduction electron and magnon Green's functions, we note the following in regard to the coupling constant I. If one assumes that the interaction, Eq. (4), is responsible for the shift in the band edge in going from the Curie temperature to very low temperatures, then $IS/2$ should be equivalent to the observed shift in the band edge. Experimental measurements reviewed by Methfessel and Mattis[9] indicate that the band edge shifts by 0.2 eV in EuO, for example, between the Curie temperature and very low temperatures, which gives $I \cong 0.1$ eV. Resistivity measurements of the spin-disorder scattering, however, indicate that I may be somewhat smaller, $I \cong 0.05$ eV. For the numerical work presented in this paper, we chose $I = 0.1$ eV. A different choice for I leads to a different splitting of the conduction bands and gives rise to somewhat different results from those given in this paper.

III. GREEN'S FUNCTIONS

The real-time thermodynamic electron Green's function is defined as

$$G_\sigma(\vec{k}, \tau) = -i \,\mathrm{Tr}\{\rho T_\tau [c_{\vec{k},\sigma}(\tau)\, c^\dagger_{\vec{k},\sigma}(0)]\} , \tag{9}$$

where $$\rho = \frac{\exp[-\beta(\mathcal{H} - \mu\mathfrak{N})]}{\mathrm{Tr}\{\exp[-\beta(\mathcal{H} - \mu\mathfrak{N})]\}} \tag{10}$$

and $\mathfrak{N}$ is the number operator for the conduction electrons.

This Green's function has been calculated by two methods. In the first method, the spin operators in the Hamiltonian, Eq. (6), are expanded in terms of magnon creation and annihilation operators, keeping in $\mathcal{H}$ only terms bilinear in the magnon operators. Although these operators have convenient commutation relations, their use is restricted to low temperatures. A magnon temperature Green's function is defined in terms of these operators, and the electron-magnon problem treated in a way analogous to the electron-phonon problem. Feynman rules for calculating the electron temperature Green's function to arbitrary orders have been derived, and the electron Green's function has been explicitly calculated to second order in the interaction using these rules. The second method keeps the spin operators in the Hamiltonian, without substituting magnon operators. A temperature Green's function for spins is defined, and the perturbation theory of Giovannini, Peter, and Koide[10] is used to obtain the electron Green's function. Although a very tedious calculation in general, the electron Green's function has been calculated to second order in the interaction using this approach. The details of both of these calculations are given elsewhere[11]; the results of the two calculations differ only by terms which are small at low temperatures. The

electron Green's function at low temperatures is given approximately by

$$\mathrm{Re}G_\sigma(\vec{k},\epsilon) = \frac{\hbar[\epsilon-(\tilde{\epsilon}_{\vec{k},\sigma}-\mu)-\hbar\Sigma_{1,\sigma}(\vec{k},\epsilon)]}{[\epsilon-(\tilde{\epsilon}_{\vec{k},\sigma}-\mu)-\hbar\Sigma_{1,\sigma}(\vec{k},\epsilon)]^2+[\hbar\Sigma_{2,\sigma}(\vec{k},\epsilon)]^2}, \tag{11}$$

$$\mathrm{Im}G_\sigma(\vec{k},\epsilon) = -\hbar^2\tanh\tfrac{1}{2}(\beta\epsilon) \times \frac{\Sigma_{2,\sigma}(\vec{k},\epsilon)}{[\epsilon-(\tilde{\epsilon}_{\vec{k},\sigma}-\mu)-\hbar\Sigma_{1,\sigma}(\vec{k},\epsilon)]^2+[\hbar\Sigma_{2,\sigma}(\vec{k},\epsilon)]^2}, \tag{12}$$

where

$$\Sigma_{1,+}(\vec{k},\epsilon) = \frac{SI^2}{2N\hbar}P\sum_{\vec{q}}\frac{\langle n_{\vec{k}+\vec{q},+}\rangle+\langle n_{\vec{q}}\rangle}{\epsilon-(\tilde{\epsilon}_{\vec{k}+\vec{q},-}-\mu)+\omega_{\vec{q}}}, \tag{13}$$

$$\Sigma_{1,-}(\vec{k},\epsilon) = \frac{SI^2}{2N\hbar}P\sum_{\vec{q}}\frac{1-\langle n_{\vec{k}-\vec{q},+}\rangle+\langle n_{\vec{q}}\rangle}{\epsilon-(\tilde{\epsilon}_{\vec{k}-\vec{q},+}-\mu)-\omega_{\vec{q}}}, \tag{14}$$

$$\Sigma_{2,+}(\vec{k},\epsilon) = \frac{SI^2\pi}{2N\hbar}\sum_{\vec{q}}(\langle n_{\vec{k}+\vec{q},-}\rangle+\langle n_{\vec{q}}\rangle)\,\delta[\epsilon-(\tilde{\epsilon}_{\vec{k}+\vec{q},-}-\mu)+\omega_{\vec{q}}], \tag{15}$$

$$\Sigma_{2,-}(\vec{k},\epsilon) = \frac{SI^2\pi}{2N\hbar}\sum_{\vec{q}}(1-\langle n_{\vec{k}-\vec{q},+}\rangle+\langle n_{\vec{q}}\rangle) \times\delta[\epsilon-(\tilde{\epsilon}_{\vec{k}-\vec{q},+}-\mu)-\omega_{\vec{q}}]. \tag{16}$$

P denotes the principal value, and it is understood that the sums in Eqs. (13)–(16) are to be evaluated by converting to integrals. $\tilde{\epsilon}_{\vec{k},\sigma}$ is defined by Eq. (8) and $\omega_{\vec{q}}$ is given by

$$\omega_{\vec{q}} = \omega_0+2ZJS[1-(1/Z)\textstyle\sum_{\vec{\delta}}e^{i\vec{q}\cdot\vec{\delta}}]. \tag{17}$$

Dyson's equation for the temperature Green's function, $_\sigma(\vec{k},\epsilon_n)$, from which the real-time Green's function given above was obtained, is shown in Fig. 1. The processes giving rise to the above self-energies are shown in the time-ordered diagrams of Figs. 2 and 3, for up and down moments, respectively. Note that the processes illustrated in Figs. 2(b) and 3(b) depend on the presence of magnons in the initial state, and hence cannot occur at zero temperature. The process shown in Fig. 2(a) depends on the creation of a hole for the intermediate state, and thus can take place only in the presence of down moments in the initial state.

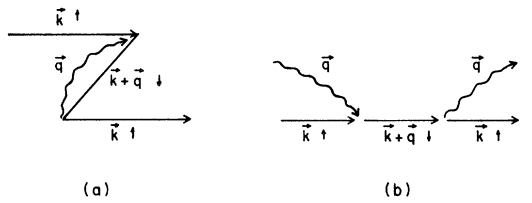

FIG. 2. Time-ordered diagrams of the two processes contributing to the self-energy of up-moment conduction electrons.

The corrected electron energy $\mathcal{E}_{\vec{k},\sigma}$ and the electron lifetime due to magnon scattering, $\tau_{\vec{k},\sigma}$, are given approximately by

$$\mathcal{E}_{\vec{k},\sigma} = \tilde{\epsilon}_{\vec{k},\sigma}+\hbar\Sigma_{1,\sigma}(\vec{k},\tilde{\epsilon}_{\vec{k},\sigma}-\mu), \tag{18}$$

$$\frac{1}{\tau_{\vec{k},\sigma}} = \frac{\Sigma_{2,\sigma}(\vec{k},\tilde{\epsilon}_{\vec{k},\sigma}-\mu)}{1-\hbar\partial\Sigma_{1,\sigma}(\vec{k},\epsilon)/\partial\epsilon\,|_{\epsilon=\tilde{\epsilon}_{\vec{k},\sigma}-\mu}}. \tag{19}$$

The corrected electron energy, Eq. (18) together with Eqs. (13) and (14), is essentially identical with the perturbation-theory result obtained by Vonsovskii and Izyumov[6] for the case of a transition metal. This result is also similar to that obtained for a rare-earth metal by Cole and Turner,[7] although Cole and Turner neglected the terms in Eqs. (13) and (14) involving $\langle n_{\vec{q}}\rangle$.

The real-time thermodynamic magnon Green's function, under the assumption that the spin operators in the Hamiltonian [Eq. (6)] may be expanded in terms of magnon operators, keeping only bilinear terms, is

$$D(\vec{q},\tau) = -i\,\mathrm{Tr}\{\rho T_\tau[a_{\vec{q}}(\tau)\,a_{\vec{q}}^\dagger(0)]\}, \tag{20}$$

where ρ is defined in Eq. (10). This Green's function has been calculated to second order in the interaction and for low temperatures is given

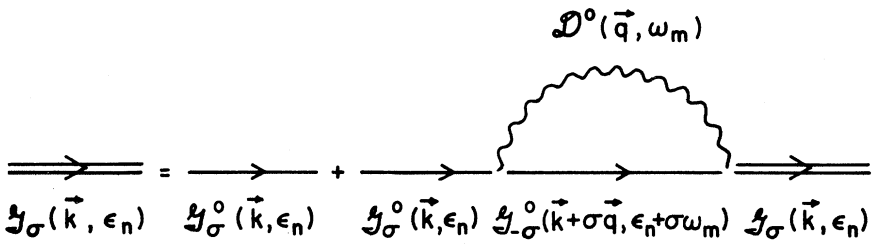

FIG. 1. Dyson's equation for the electron temperature Green's function from which the real-time Green's function given in this paper was obtained. The magnon Green's function in this figure is directed to the left for up moments and to the right for down moments. $\epsilon_n = (2n+1)\pi/\beta$, $\omega_m = 2m\pi/\beta$, where n and m are integers.

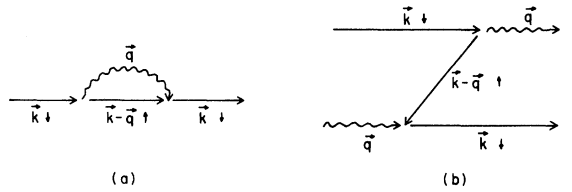

FIG. 3. Time-ordered diagrams of the two processes contributing to the self-energy of down-moment conduction electrons.

by

$$\mathrm{Re}D(\vec{q},\omega)=\frac{\hbar[\omega-\omega_{\vec{q}}-\hbar\Pi_1(\vec{q},\omega)]}{[\omega-\omega_{\vec{q}}-\hbar\Pi_1(\vec{q},\omega)]^2+[\hbar\Pi_2(\vec{q},\omega)]^2}, \tag{21}$$

$$\mathrm{Im}D(\vec{q},\omega)=-\hbar^2\coth\tfrac{1}{2}(\beta\omega)\times\frac{\Pi_2(\vec{q},\omega)}{[\omega-\omega_{\vec{q}}-\hbar\Pi_1(\vec{q},\omega)]^2+[\hbar\Pi_2(\vec{q},\omega)]^2}, \tag{22}$$

where $$\Pi_1(\vec{q},\omega)=\frac{SI^2}{2N\hbar}P\sum_{\vec{k}}\frac{\langle n_{\vec{k}-\vec{q},+}\rangle-\langle n_{\vec{k},-}\rangle}{\omega_{\vec{q}}+\tilde{\epsilon}_{\vec{k}-\vec{q},+}-\tilde{\epsilon}_{\vec{k},-}}, \tag{23}$$

$$\Pi_2(\vec{q},\omega)=\frac{SI^2\pi}{2N\hbar}\sum_{\vec{k}}(\langle n_{\vec{k}-\vec{q},+}\rangle-\langle n_{\vec{k},-}\rangle)\,\delta[\omega_{\vec{q}}+\tilde{\epsilon}_{\vec{k}-\vec{q},+}-\tilde{\epsilon}_{\vec{k},-}]. \tag{24}$$

Dyson's equation for the temperature Green's function, $\mathfrak{D}(\vec{q},\omega_n)$, from which the real-time Green's function given above was obtained, is shown in Fig. 4.

The corrected magnon energy $\mathfrak{w}_{\vec{q}}$ and the magnon lifetime due to the electron-magnon interaction, $\tau_{\vec{q}}$, are given by expressions similar to Eqs. (18) and (19) but with $\omega_{\vec{q}}$ and $\Pi(\vec{q},\omega_{\vec{q}})$ in place of $\tilde{\epsilon}_{\vec{k},\sigma}$ and $\Sigma(\vec{k},\epsilon_{\vec{k},\sigma}-\mu)$ in those expressions.

In the following sections, we shall apply the above-derived expressions to evaluate certain physical properties of the electron-magnon system. We shall use parameters that are characteristic of a typical material such as europium oxide.

IV. ELECTRON AND MAGNON ENERGY CORRECTION

In this section we numerically evaluate electron and magnon energy corrections arising from the electron-magnon interaction. These quantities will then be used to evaluate the electron effective mass and the specific heat of both the electron and magnon systems.

In order to evaluate the electron-energy correction we shall approximate the ferromagnetic magnon spectrum in a lattice with cubic-crystal structure by a quadratic dispersion relation with a wave-vector cutoff q_m

$$\omega_{\vec{q}}\to\tilde{\omega}_{\vec{q}}=\omega_0+2JSa^2q^2,\quad q<q_m \tag{25}$$

where a is the distance between nearest magnetic neighbors. This approximation does not significantly affect the results, provided that q_m is chosen such that $\frac{4}{3}\pi q_m^3$ is equal to the volume of the first Brillouin zone of the reciprocal lattice. The sum over $\vec{q}$ contained in Eq. (18) is evaluated by converting to an integral. Defining the variable $\vec{l}=\vec{k}+\sigma\vec{q}$ and choosing the polar axis of the $\vec{l}$ integration to lie along $\vec{k}$, the energy correction becomes

$$\begin{aligned}\Delta\mathcal{E}_{\vec{k},\sigma}&=\mathcal{E}_{\vec{k},\sigma}-\tilde{\epsilon}_{\vec{k},\sigma}\\&=\frac{SI^2}{2N}\frac{2\pi\Omega}{(2\pi)^3}P\int_{-1}^{1}du\int_0^{l_m(u)}l^2dl\\&\quad\times\{\tfrac{1}{2}(1-\sigma)+\sigma[\exp(\beta\tilde{\epsilon}_{\vec{l},-\sigma}-\mu)+1]^{-1}\\&\quad+[\exp(\beta\tilde{\omega}_{\vec{k}-\vec{l}})-1]^{-1}\}\left(\frac{\hbar^2k^2}{2m}-\frac{\hbar^2l^2}{2m}\right.\\&\quad\left.+\sigma[\omega_0+2JSa^2(k^2-2klu+l^2)-IS-2\mu_BH]\right)^{-1},\end{aligned} \tag{26}$$

where $$l_m(u)=ku+[q_m^2-(1-u^2)k^2]^{1/2}. \tag{27}$$

In the case of zero temperature, the electron-energy correction has been evaluated analytically, but in general, Eq. (26) must be evaluated numerically, taking the principle value of the integral in cases where the integrand diverges. Typical examples of the electron-energy corrections in the vicinity of the Fermi level are shown in Fig. 5, using the parameters given in Table I. The energy corrections shown in the figure are for up moments at a doping of 4.56×10^{20} (conduction elec-

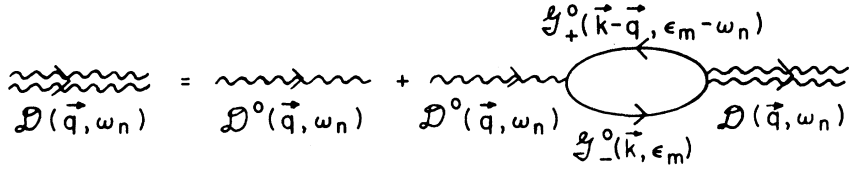

FIG. 4. Dyson's equation for the magnon-temperature Green's function from which the real-time Green's function given in this paper was obtained. $\omega_n=2n\pi/\beta$, $\epsilon_m=(2m+1)\pi/\beta$, where n and m are integers.

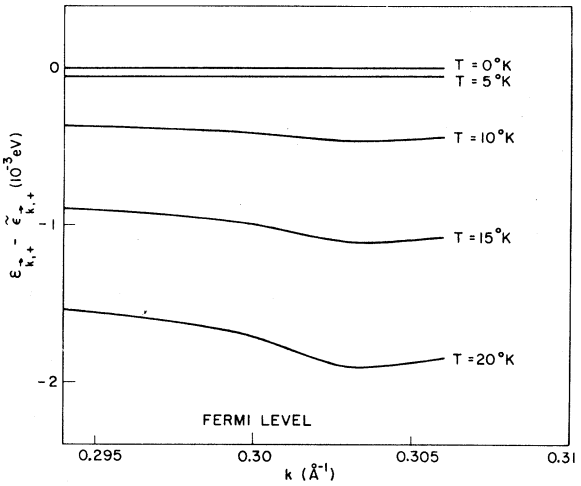

FIG. 5. Electron-energy correction as a function of electron wave vector in the vicinity of the Fermi level, for up-moment conduction electrons in a magnetic semiconductor with parameters given in Table I. $n = 4.56 \times 10^{20}$ (conduction electrons)/cm^3.

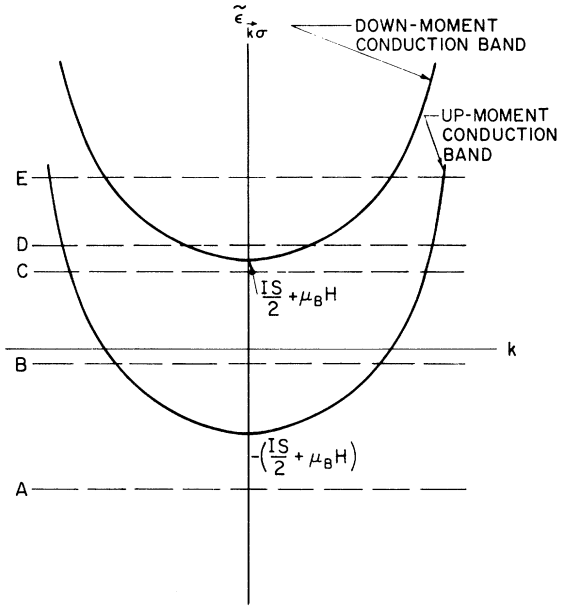

FIG. 6. Assumed conduction-electron band structure, $\tilde{\epsilon}_{\vec{k},\sigma}$, as given by Eq. (8). The conduction-electron localized moment coupling constant is taken to be positive. Dashed lines show various possible Fermi levels which arise from variation of the doping.

trons)/cm^3. At this value of doping, there is a well defined and relatively large up-moment Fermi sphere, but the Fermi level is below the band edge of the down moments (i.e., a Fermi level at line C of Fig. 6) and hence there are very few down-moment conduction electrons at low temperatures.

If the doping is somewhat greater so that a well-defined down-moment Fermi sphere exists, then the zero-temperature electron-energy correction for up moments would *not* be zero as it is in Fig. 5, since the presence of many down-moment conduction electrons allows the process illustrated in Fig. 2(a) readily to take place. Further, in such cases of heavier doping, the zero-temperature curves of the energy correction as a function of wave vector would show two logarithmic singularities just below the Fermi level. This is an indication that higher-order terms in the perturbation expansion must be treated at wave vectors where here is such a singularity. These logarithmic singularities, however, are "smoothed out" at finite temperatures. The behavior of the up-moment electron-energy correction in the case of doping heavy enough for both up- and down-moment Fermi surfaces to exist is illustrated in Fig. 7 for a hypothetical magnetic semiconductor whose parameters are given in Table II.

For down moments with doping large enough for a down-moment Fermi sphere to exist, the electron-energy correction is on the order of -10^{-2} to -10^{-3} eV in the vicinity of the Fermi level. At zero temperature, there are generally two logarithmic singularities as a function of wave vector above the Fermi level, which are smoothed out as the temperature is raised.

The magnon spectrum in the presence of the electron-magnon interaction, $\mathcal{W}_{\vec{q}}$, has been evaluated analytically.[11] A typical example of the magnon spectrum is shown in Fig. 8, using the parameters given in Table I and taking the doping to be 4.56×10^{20} (conduction electrons)/cm^3. Figure 8 gives three curves for the magnon-dispersion relation: the noninteracting spectrum ($g\mu_B H + 2JSa^2q^2$), the spectrum upon treating the z-component terms in $\mathcal{H}_{\text{int}}$ in the random-phase approximation ($\tilde{\omega}_{\vec{q}}$), and the corrected magnon spectrum $[\mathcal{W}_{\vec{q}} = \tilde{\omega}_{\vec{q}} + \hbar\Pi_1(\vec{q}, \tilde{\omega}_{\vec{q}})]$. At low temperatures $\mathcal{W}_{\vec{q}}$ is essentially independent of temperature. As a function of doping, the noninteracting and corrected magnon-dispersion relations have essentially the same zero wave-vector value, but the corrected magnon spectrum always increases with q more

TABLE I. Parameters characteristic of a typical ferromagnetic semiconductor such as europium oxide. The magnetic lattice is fcc.

$a = 3.64$ Å	$g = 2$
$T_c = 76$ °K	$q_m = 1.203$ Å^{-1}
$J = 1.04 \times 10^{-4}$ eV	$I = 0.1$ eV
$S = \frac{7}{2}$	$H = 10\,000$ G

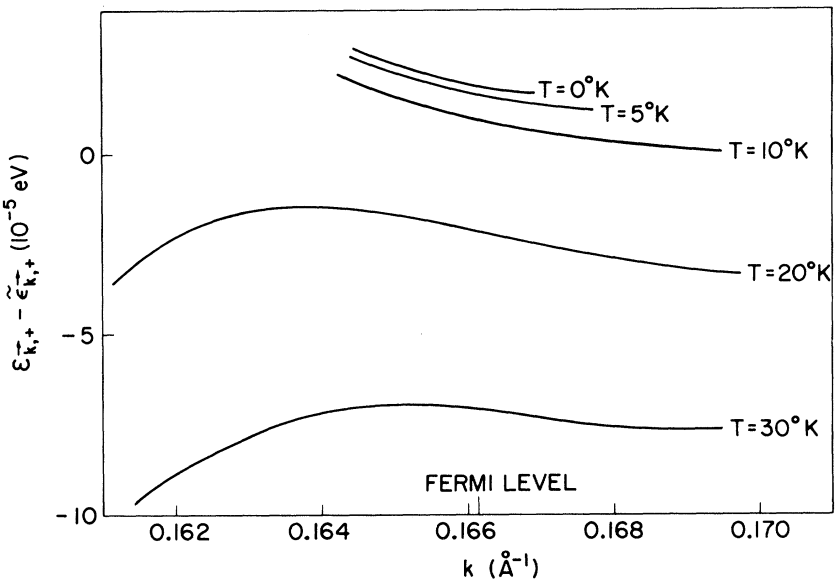

FIG. 7. Electron-energy correction as a function of electron wave vector in the vicinity of the Fermi level, for up-moment conduction electrons in a hypothetical magnetic semiconductor with parameters given in Table II. The $T=0$ °K curve diverges logarithmically at two wave vectors slightly smaller than the wave vectors shown in the figure.

rapidly than the noninteracting spectrum.

An analysis of the structure of higher-order terms in the perturbation expansion of the Green's functions and a consideration of the magnitudes of the corrections calculated in this section indicates that with the exception of the zero-temperature singularities noted above, the results given here are quite similar to those that would be obtained from an exact treatment of the problem. This is justification for using only second-order terms in the calculation of the self-energy.

V. ELECTRON EFFECTIVE MASS

As a result of the emission and reabsorption of magnons, each conduction electron is surrounded by a cloud of virtual magnons, which affects the response of the electron to an external electric field. The response of such an electron may be characterized by an effective mass defined by

$$m^* = \frac{\hbar^2 k}{\partial \mathcal{E}_{\vec{k},\sigma}/\partial k} \quad . \tag{28}$$

This definition of the effective mass is appropriate for electrons which are away from the botton of the conduction band; for electrons which are near the bottom of the band the effective mass is defined in terms of the second derivative of the corrected electron energy.

The effective mass at the Fermi level is numerically evaluated by approximating the derivative in Eq. (28) by a difference expression. Typical results for the effective mass are shown in Figs. 9, 10, and 11 for the parameters of Table I.

Figure 9 gives the effective mass at the Fermi level as a function of doping, at $T=10$ °K. For dopings in the range from 4.6 to 4.75×10^{20} (conduction electrons)/cm^3, the up-moment effective mass at the Fermi level varies rapidly as a function of doping. The up-moment effective masses are very different from the down-moment effective masses. Also, for given doping greater than 4.6×10^{20} (conduction electrons)/cm^3, the effective mass varies substantially as a function of wave vector in the vicinity of the Fermi level, as illustrated in Fig. 10. This reflects the distortion of the energy-momentum relation near the Fermi level.

Figure 11 gives the effective mass at the Fermi level as a function of temperature for a doping of 8.15×10^{20} (conduction electrons)/cm^3. Immediately below (above) the Fermi level the up-moment effective mass for $T\lesssim10$ °K is increased (decreased) and the down-moment effective mass for $T\lesssim10$ °K is decreased (increased) from that shown in the figure. For $T\gtrsim10$ °K the effective masses remain approximately as shown in the figure as wave vector is varied in the immediate vicinity of the Fermi level.

TABLE II. Parameters for a hypothetical magnetic semiconductor used in the numerical computations presented in this paper. The magnetic lattice is simple cubic.

$a=3.14$ Å	$g=2$
$T_c=464$ °K	$q_m=1.24$ Å^{-1}
$J=0.01$ eV	$I=0.1$ eV
$S=1$	$H=10\,000$ G
$n=7.83\times10^{19}$ (conduction electrons)/cm^3	

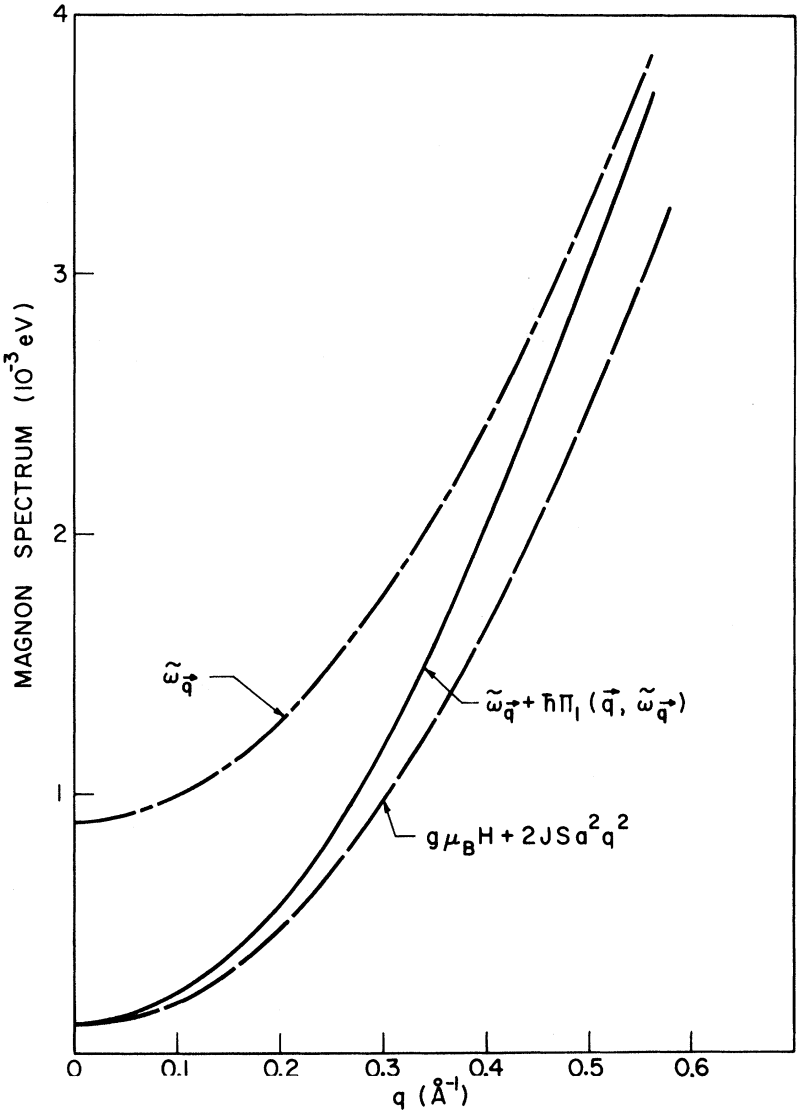

FIG. 8. Low-temperature magnon spectrum as a function of magnon wave vector. Dashed line is the noninteracting spectrum; dot-dashed line is the spectrum upon treating the z-component terms in $\mathcal{H}_{int}$ in the random-phase approximation; solid line is the corrected magnon spectrum. $n = 4.56 \times 10^{20}$ (conduction electrons)/cm^3.

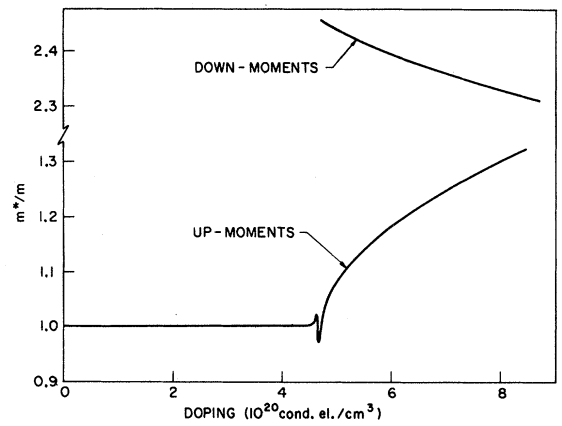

FIG. 9. Effective mass at the Fermi level as a function of doping, for up and down moments in a magnetic semiconductor with parameters given in Table I. $T = 10\,^\circ$K.

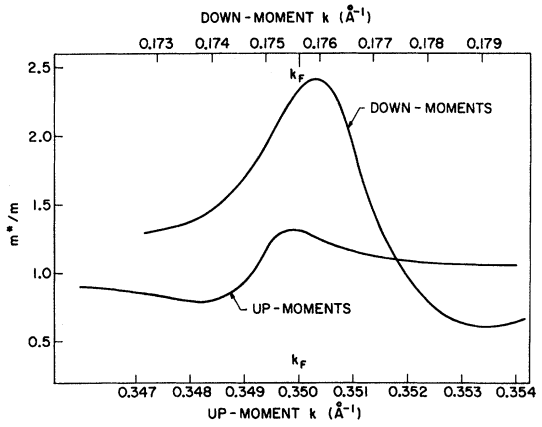

FIG. 10. Effective mass as a function of wave vector, for up and down moments in a magnetic semiconductor with parameters in Table I. $T = 10\,^\circ$K. $n = 8.15 \times 10^{20}$ (conduction electrons)/cm^3.

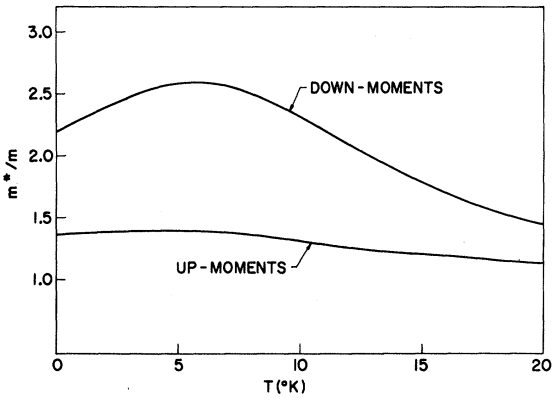

FIG. 11. Effective mass at the Fermi level as a function of temperature, for up and down moments in a magnetic semiconductor with parameters in Table I. $n = 8.15 \times 10^{20}$ (conduction electrons)/cm^3.

The value of doping, above which the effects discussed in the previous paragraphs are important, depends critically on the coupling constant I, as this coupling constant determines the magnitude of the conduction band splitting and hence determines the doping above which down moments will be present in the sample. Thus, if I is varied from 0.1 eV, the values of doping quoted in this paper must be varied accordingly. The effects discussed above depend also on the coupling constant J. As J is increased, m^*/m comes closer to unity and shows less variation with wave vector and doping. For instance, m^*/m at the Fermi level for the parameters of Table II differs from unity by less than 1%.

Note that both up- and down-moment effective masses are shifted as a result of the electron-magnon interaction, and that the behavior of the up-moment effective mass as a function of tem-

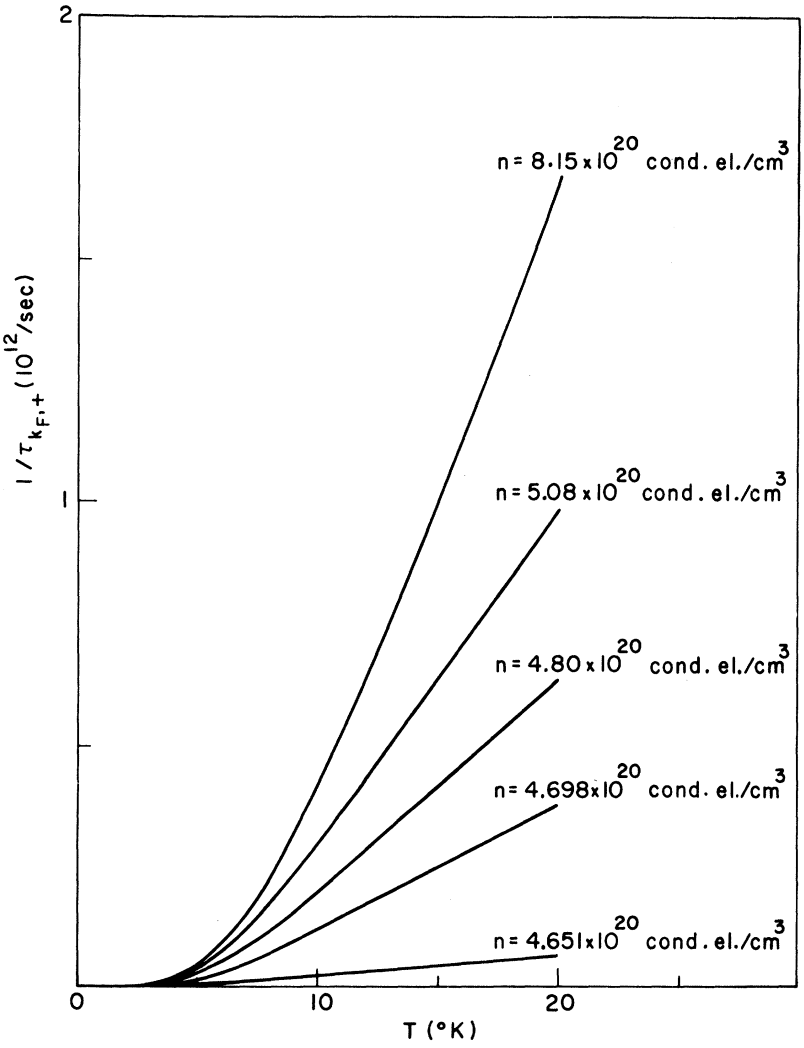

FIG. 12. Electron lifetime due to magnon scattering at the Fermi level, for up moments in a magnetic semiconductor with parameters given in Table I.

perature and wave vector is quite different from that of the down-moment effect mass. This is slightly different from the conclusion reached in our earlier paper,[5] where we argued that the processes contributing to the up-moment effective-mass correction were frozen out at zero temperature. Cole[12] has also noted that both electron polarizations will be effected by the electron-magnon interaction. This behavior of the effective mass will be important when we consider the conduction-electron mobility in Sec. VII.

VI. ELECTRON AND MAGNON LIFETIME

The electron lifetime due to magnon scattering, Eq. (19), may be evaluated analytically if the magnon spectrum as given in Eq. (25) is used and if the denominator in Eq. (19) is taken to be 1.[11] The latter assumption is generally quite valid at the Fermi level for the cases considered in this paper.

Reciprocal lifetimes at the Fermi level are given for up and down movements in Figs. 12 and 13, using the parameters given in Table I. These curves show the lifetime as a function of temperature for various dopings. Note that for doping below about 4.65×10^{20} (conduction electrons)/cm^3, the up-moment reciprocal lifetime at the Fermi level is zero at all low temperatures. For such dopings there are essentially no down moments, and the Fermi level is low enough that the energy-conserving δ function contained in Eq. (19) can never be satisfied. At somewhat larger dopings the reciprocal lifetime is large, and magnon scattering may then be a dominant contribution to the electron lifetime in magnetic semiconductors. For down moments, the reciprocal lifetime at the Fermi level is large, but the Fermi level is above the down-moment band edge (e.g., at line D of Fig. 6) only for doping larger than about 4.68

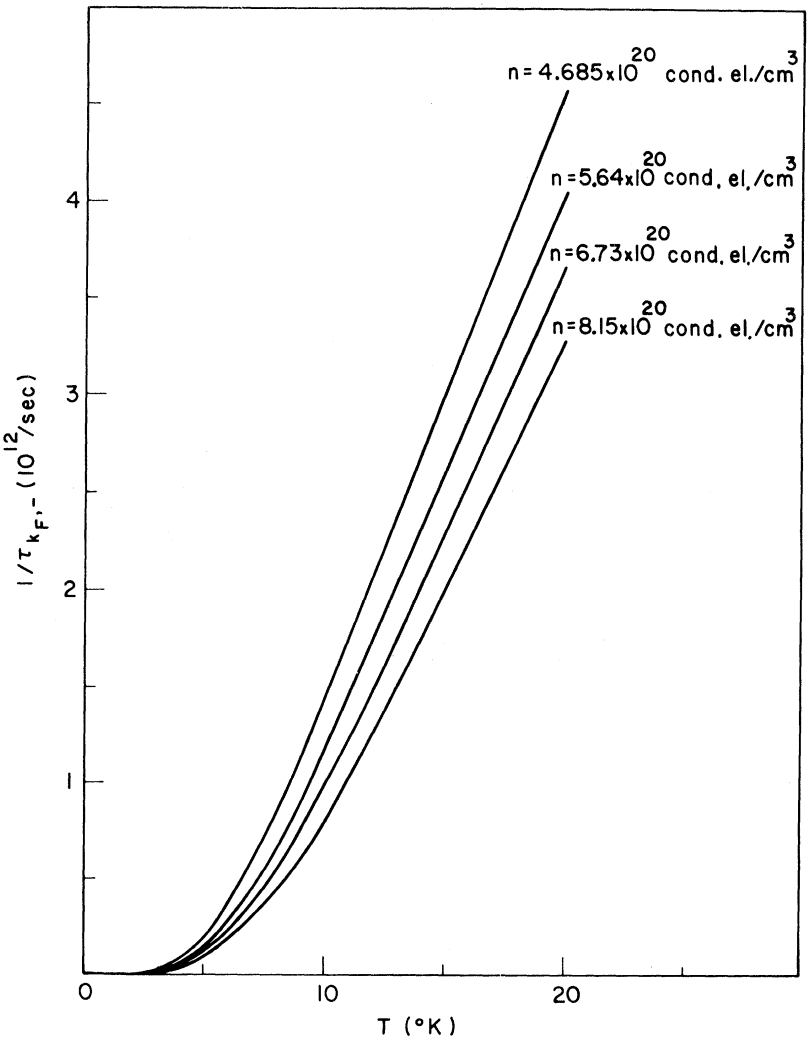

FIG. 13. Electron lifetime due to magnon scattering at the Fermi level, for down moments in a magnetic semiconductor with parameters given in Table I.

$\times 10^{20}$ (conduction electrons)/cm^3, so lifetimes at the Fermi level are calculated only for these dopings. Note that the reciprocal lifetime becomes roughly linear in the temperature above a minimum T.

The magnon lifetime due to interaction with conduction electrons has been calculated analytically using the same approximations made in the evaluation of the conduction-electron lifetime.[11]

Figure 14 shows curves of the magnon lifetime for several dopings at 10°K for the case of Table I. There are several interesting features of the lifetime. The lifetime as a function of wave vector is very strongly dependent on doping. Above a doping of approximately 4.7×10^{20} (conduction electrons)/cm^3, the magnon lifetime is essentially independent of temperature.

The lifetime is quite strongly peaked around the magnon wave vectors which conserve momentum in the processes contributing to the energy corrections given earlier in this paper; the curves of Fig. 14 indicate quite clearly the range of magnon wave vectors which are important in the renormalization processes. Thus, in some sense, the curves of reciprocal lifetime may be considered as curves of the weighting function for the wave vectors of the magnons which dress the conduction electrons, and the inverse Fourier transform of

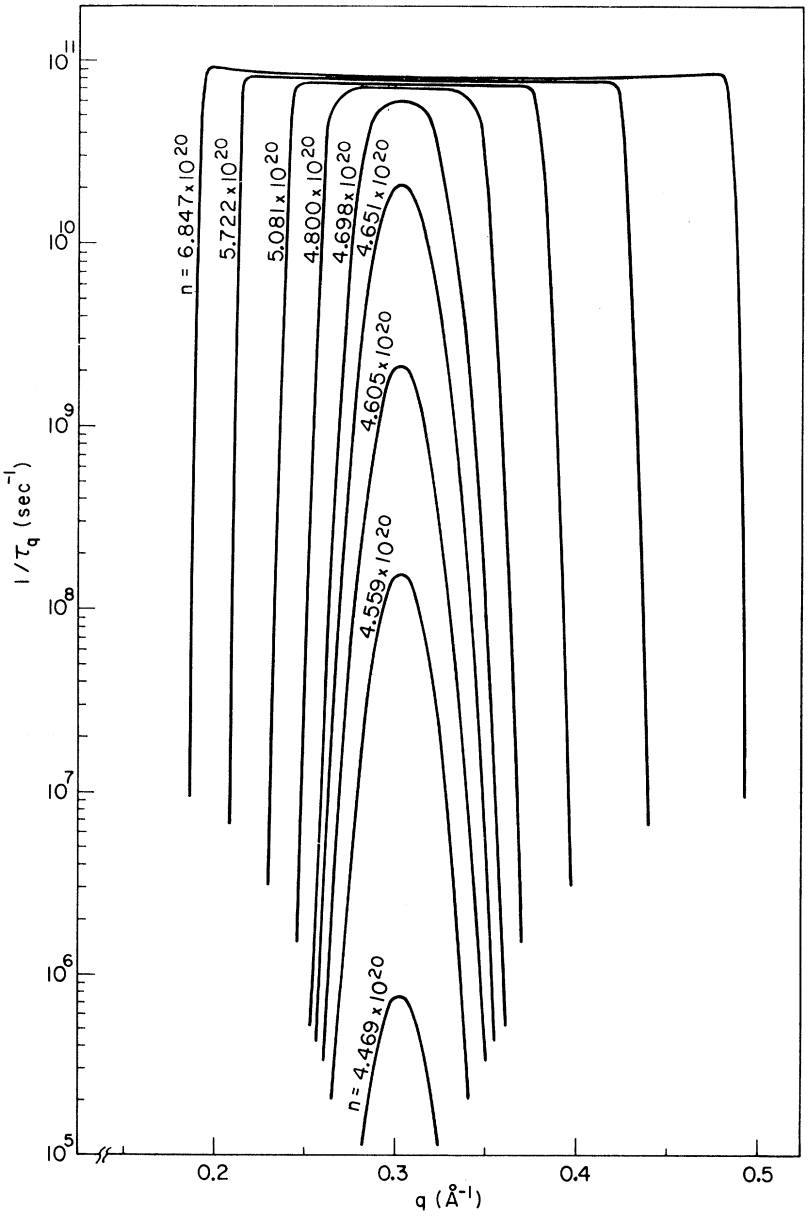

FIG. 14. Magnon lifetime due to the electron-magnon interaction, for a magnetic semiconductor with parameters given in Table I. $T=10$ °K. Doping [in (conduction electrons)/cm^3] is indicated for each curve.

this weighting function should give an estimate of the spatial extent of the interaction between conduction electrons and ionic moments. The size of the magnetic polaron arising from this interaction is thus estimated to be on the order of 50 to 100 Å.

It should be emphasized that the effects considered in this section depend quite strongly on the doping, and, in turn, on the coupling constant I. A variation in I leads to different values of doping at which the effects discussed in this section take place.

VII. ELECTRON MOBILITY

The conduction-electron mobility at the Fermi level under the electron-magnon interaction

$$\mu = e\tau/m^* \tag{29}$$

may be obtained by combining our results for the effective mass and the lifetime. For up moments, this mobility is infinite at dopings less than about 4.65×10^{20} (conduction electrons)/cm^3, because $\tau_{k_F,+}$ is infinite; for these dopings the mobility is governed entirely by other mechanisms. At higher dopings, where both up and down moments are present, the mobility at the Fermi level shows very interesting behavior as a function of temperature as illustrated in Fig. 15, first decreasing rapidly as T is raised from zero due to $\tau_{k_F,+}$ decreasing, and then tending to decrease much less rapidly, due partly to the behavior of m^*. The up-moment mobility is a much stronger function of doping than the down-moment mobility; it decreases quite rapidly as the doping is raised, due to the decrease in the up-moment electron lifetime.

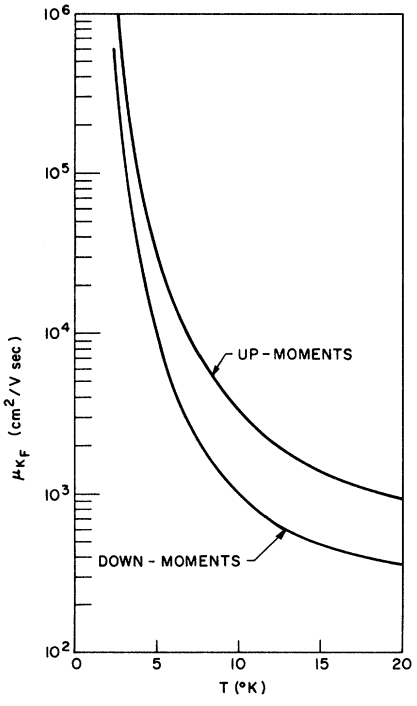

FIG. 15. Conduction-electron mobility under the electron-magnon interaction for up and down moments in a magnetic semiconductor with parameters given in Table I. $n = 8.15\times10^{20}$ (conduction electrons)/cm^3.

This behavior for the mobility is true at the Fermi level. Since the effective mass is a strong function of wave vector in the vicinity of the Fermi level, however, the mobility will also be a strong function of wave vector. We must take this variation in mobility into account and consider all other processes which contribute to electron mobility in computing the average mobility of conduction electrons in a magnetic semiconductor. Since this average should generally be different for up and down moments, a magnetic Gunn effect[13] may be possible in magnetic semiconductors.

VIII. SPECIFIC HEAT

The specific heat of a typical magnetic semiconductor arises from several sources; among these are contributions from conduction electrons, magnons, and phonons. In the absence of interactions, the behavior of these contributions is well-known. The contribution to the specific heat from the conduction electrons varies linearly with T, provided that the Fermi level is well above the band edge of both up- and down-moment conduction electrons. The contribution from the magnons varies as $T^{3/2}$ if the external magnetic field is small enough that the magnon energy is essentially zero for zero magnon wave vector. The phonon contribution varies as T^3 and is small compared with the electronic contribution at low enough temperatures. In this section we calculate the conduction electron and magnon specific heats in the presence of the electron-magnon interaction, and we show that the magnon contribution is large. This contribution is much more important than the phonon contribution at low temperatures.

The magnon contribution to the specific heat is given by

$$c_{v,\,\mathrm{mag}} = \frac{1}{2\pi^2 k_B T^2}\int_0^{q_m} \frac{q^2 \mathfrak{w}_{\vec{q}}^2 \exp(\beta\mathfrak{w}_{\vec{q}})\,dq}{(\exp(\beta\mathfrak{w}_{\vec{q}})-1)^2} \tag{30}$$

and is plotted in Fig. 16 for the case of Table I with the doping of 4.56×10^{20} (conduction electrons)/cm^3. The magnon specific heats using the other magnon-dispersion relations given in Fig. 8 are also plotted in Fig. 16. Note that the noninteracting and corrected magnon specific heats differ by approximately 20%, with the corrected spe-

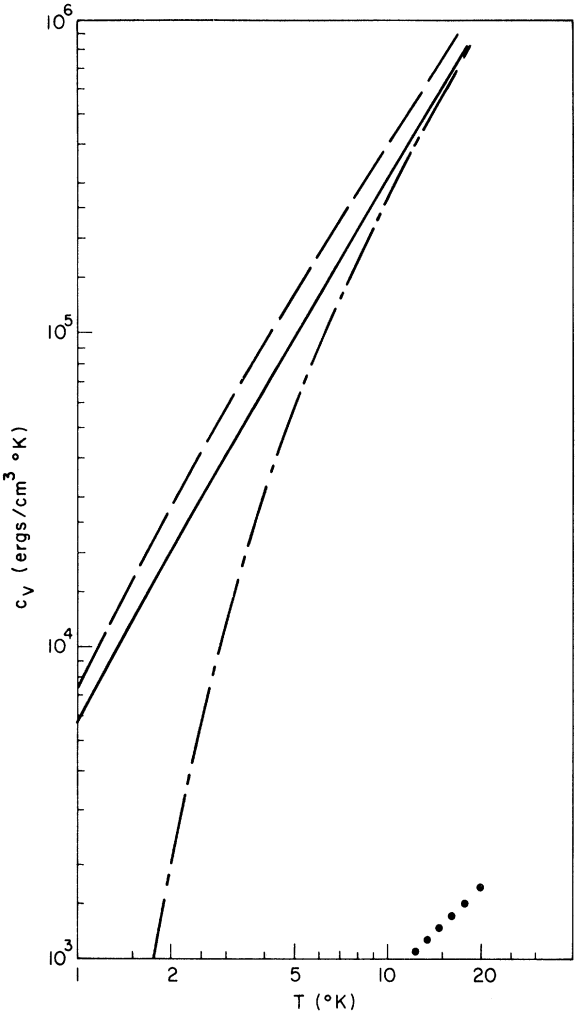

FIG. 16. Conduction-electron and magnon specific heats. Dashed line is the magnon specific heat in the absence of interactions; dot-dashed line is the magnon specific heat arising from using $\tilde{\omega}_{\vec{q}}$ as the magnon spectrum; solid line is the corrected magnon specific heat; dotted line is the corrected electronic specific heat. $n = 4.56 \times 10^{20}$ (conduction electrons)/cm^3.

cific heat being decreased from the noninteracting specific heat.

The electronic specific heat may be calculated from an equation similar to Eq. (30). The correction to the electronic specific heat may also be calculated independently. The change in entropy of the conduction electrons in a magnetic semiconductor arising from the electron-magnon interaction is given approximately by[14]

$$\Delta S_\sigma = \frac{\hbar}{T} \sum_{\vec{k}} \int_{-\infty}^{+\infty} d\epsilon\, \epsilon \frac{\partial n_\epsilon}{\partial \epsilon} \delta\left[\epsilon - (\tilde{\epsilon}_{\vec{k},\sigma} - \mu) - \hbar \Sigma_{1,\sigma}(\vec{k}, \epsilon)\right] \Sigma_{1,\sigma}(\vec{k}, \epsilon) , \tag{31}$$

where $n_\epsilon = 1/(e^{\beta\epsilon} + 1)$. (32)

The magnon contribution to the electronic specific heat is then given approximately by

$$\Delta c_{v,\,\mathrm{elect}} = \frac{\hbar T}{2\pi^2} \times \sum_\sigma \int_0^\infty k^2\, dk \frac{\partial}{\partial T}\left(\frac{1}{T} \frac{\partial n_\epsilon}{\partial \epsilon} \Sigma_{1,\sigma}(\vec{k}, \epsilon)\epsilon\right)\Bigg|_{\epsilon = \tilde{\epsilon}_{\vec{k},\sigma} - \mu} . \tag{33}$$

The electronic specific heat and specific-heat correction are evaluated numerically, approximating $\Sigma_{1,\sigma}(\vec{k}, \tilde{\epsilon}_{\vec{k},\sigma} - \mu)$ by polynomials through points computed numerically using Eq. (26). Numerical results indicate that this specific heat is a few percent larger than the noninteracting specific heat. An example of the total electronic specific heat is given in Fig. 16. Note that the electronic specific heat is orders of magnitude smaller than the magnon specific heat.

IX. CONCLUSION

We have considered in this paper the effects of the conduction-electron localized moment interaction on certain physical properties of ferromagnetic semiconductors. We have treated the electron-magnon interaction in the limit of low temperatures where spin-wave theory is valid and have considered the case of the large polaron in which the spatial extent of the interaction is large.

We have found that the corrections to the properties considered can often be large in typical materials. At doping levels where there are both up and down moments, the effective mass, lifetime, and mobility of conduction electrons behave quite differently and are much more affected by the interaction than at lower dopings. Further, the magnon lifetime can change by orders of magnitude as the doping is varied. Observation of these effects can provide an excellent method for determining the conduction-electron localized moment coupling constant.

The correction to the magnon specific heat is large, and the magnon specific heat can be much more important than the phonon specific heat at low temperature. The conduction-electron specific heat and the electron-magnon correction thereto are small in magnetic semiconductors.

We further note that the results given in this paper are not only important for the low-temperature behavior they predict but are also useful in that they must be limiting values of any more general theory that treats the phenomena discussed here.

ACKNOWLEDGMENTS

One of us (R. B. W.) wishes to express his appreciation to Walter B. Hewlett and Michael J. Y. Williams for their generous assistance with the numerical computations presented in this paper.

*Work supported by the Advanced Research Projects Agench through the Center for Materials Research at Stanford University, Stanford, Calif. 94305.

†National Science Foundation Predoctoral Fellow.

[1]T. Wolfram and J. Callaway, Phys. Rev. 127, 1605 (1962).

[2]C. Haas, Phys. Rev. 168, 531 (1968).

[3]F. Rys, J. Helman, and W. Baltensperger, Physik Kondensierten Materie 6, 105 (1967).

[4]R. M. White, Phys. Rev. Letters 23, 858 (1969).

[5]R. M. White and R. B. Woolsey, Phys. Rev. 176, 908 (1968).

[6]S. V. Vonsovskii and Y. A. Izyumov, Usp. Fiz. Nauk 78, 3 (1962) [Soviet Phys. Usp. 5, 723 (1963)].

[7]H. S. D. Cole and R. E. Turner, Phys. Rev. Letters 19, 501 (1967).

[8]See, for example, D. Pines, in *Polarons and Excitons*, edited by C. G. Kuper and G. D. Whitfield (Oliver and Boyd, London, 1963).

[9]S. Methfessel and D. C. Mattis, in *Handbuch der Physik*, edited by S. Flügge (Springer, Berlin, 1968), Vol. 18/1, p. 484.

[10]B. Giovannini, M. Peter, and S. Koide, Phys. Rev. 149, 251 (1966).

[11]R. B. Woolsey, Ph.D. dissertation, Stanford University, Stanford, Calif., 1970 (unpublished).

[12]H. S. D. Cole, Phys. Letters 30A, 114 (1969).

[13]P. N. Butcher, Rept. Progr. Phys. 30, 97 (1967).

[14]A. A. Abrikosov, L. P. Gor'kov, and I. Y. Dzyaloshinskii, in *Quantum Field Theoretical Methods in Statistical Physics*, edited by D. ter Harr (Pergamon, New York, 1965), p. 188.

PHYSICAL REVIEW B VOLUME 1, NUMBER 11 1 JUNE 1970

COMMENTS AND ADDENDA

The Comments and Addenda section is for short communications which are not of such urgency as to justify publication in Physical Review Letters and are not appropriate for regular Articles. It includes only the following types of communications: (1) comments on papers previously published in The Physical Review or Physical Review Letters; (2) addenda to papers previously published in The Physical Review or Physical Review Letters, in which the additional information can be presented without the need for writing a complete article. Manuscripts intended for this section may be accompanied by a brief abstract for information-retrieval purposes. Accepted manuscripts will follow the same publication schedule as articles in this journal, and galleys will be sent to authors.

Composite Ising Lattices with Unequal Spins*

Robert H. T. Yeh
Department of Physics and Astronomy, State University of New York, Buffalo, New York 14214
(Received 30 January 1970)

The phase-transition problem of two-component composite Ising lattices with unequal spins in zero magnetic field is solved within the Bragg-Williams approximation.

We shall generalize our previous treatment of composite Ising lattices[1] to the case where spins of different components of the composite may have different magnitudes. We shall restrict ourselves to the two-component case with zero external field, although the method can easily be generalized to three or more components cases. Unless otherwise specified, we shall follow the notations of I.

Consider a two-component lattice with interaction constants ϵ_1, ϵ_2, ϵ_3,; structure parameters u_1, u_2, u_3, v_1, v_2; and spin magnitudes s_1, s_2. With zero external field, the partition function of this lattice is equal to the partition function of a lattice with same structure, but different interaction